Rupture complexity of an injection induced event: the 2016 Mw 5.1 Fairview, Oklahoma earthquake

J. A. López-Comino[1,2*] and S. Cesca[2]

[1] *KAUST, King Abdullah University of Science and Technology, Thuwal (Saudi Arabia).*

[2] *GFZ German Research Centre for Geosciences, Telegrafenberg, D-14473 Potsdam (Germany).*

**jose.lopezcomino@kaust.edu.sa*

DAVOS SCHATZALP 3rd Induced Seismicity Workshop 5 - 8 March 2019

1. INTRODUCTION

- Complex rupture processes for moderate-to-small earthquakes may reveal a dominant direction of the rupture propagation and the presence and geometry of one or more main slip patches.
- Finding and characterizing such properties is crucial to understand the nucleation and growth of induced earthquakes.
- We analyze one of the largest earthquakes linked to wastewater injection, the 2016 M_W 5.1 Fairview, Oklahoma earthquake (Figure 1) using Empirical Green's Function (EGF) techniques and decipher its source complexity.

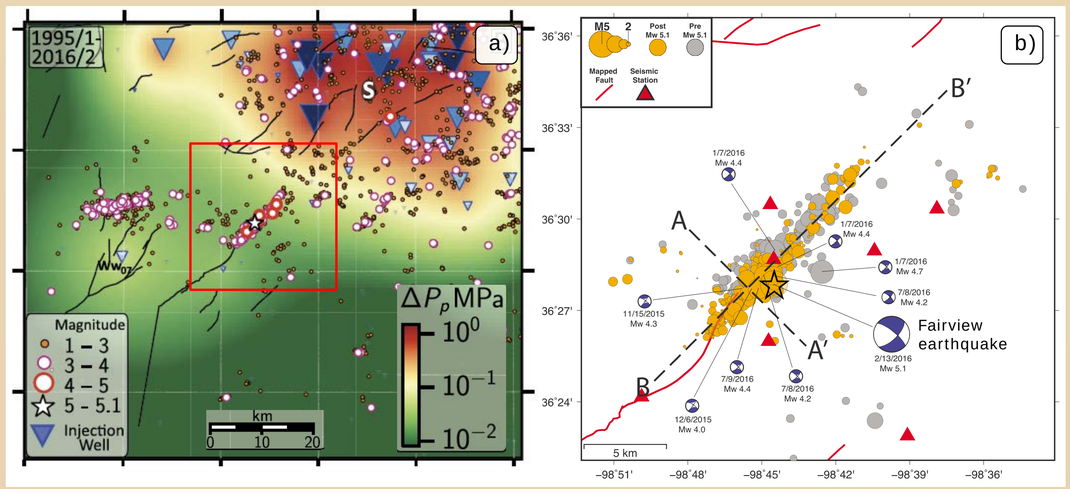

Figure 1. a) Pore pressure perturbations and seismicity at the time of the Mw 5.1 Fairview earthquake (Goebel et al., 2017). b) Relocated earthquakes in the Fairview sequence (April 2013 to 1 May 2016), including earthquakes prior to the 13 February Mw 5.1 event (gray) and those after (orange), (Yeck et al., 2016).

2. APPARENT SOURCE TIME FUNCTIONS (ASTFs) ANALYSIS

- The earthquake source for the mainshock can be isolated from seismograms through a deconvolution procedure between the mainshock and EGF waveforms, thus obtaining the Apparent Source Time Functions (ASTFs) (Figure 2a).
- Frequency domain deconvolution is performed through spectral division using S wave windows.
- Stable ASTFs are observed for different EGFs revealing the source complexity of the target earthquake (Figure 2b).

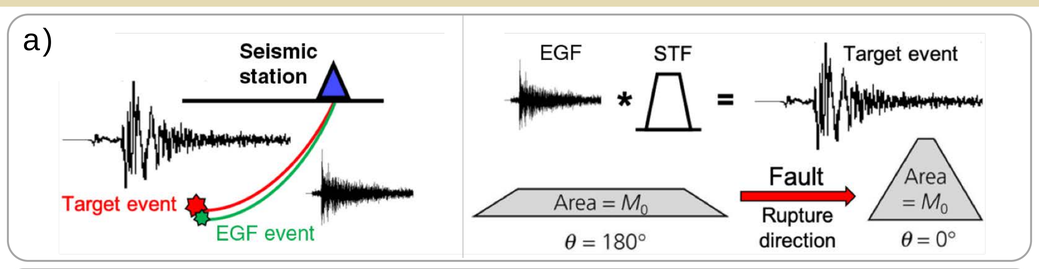

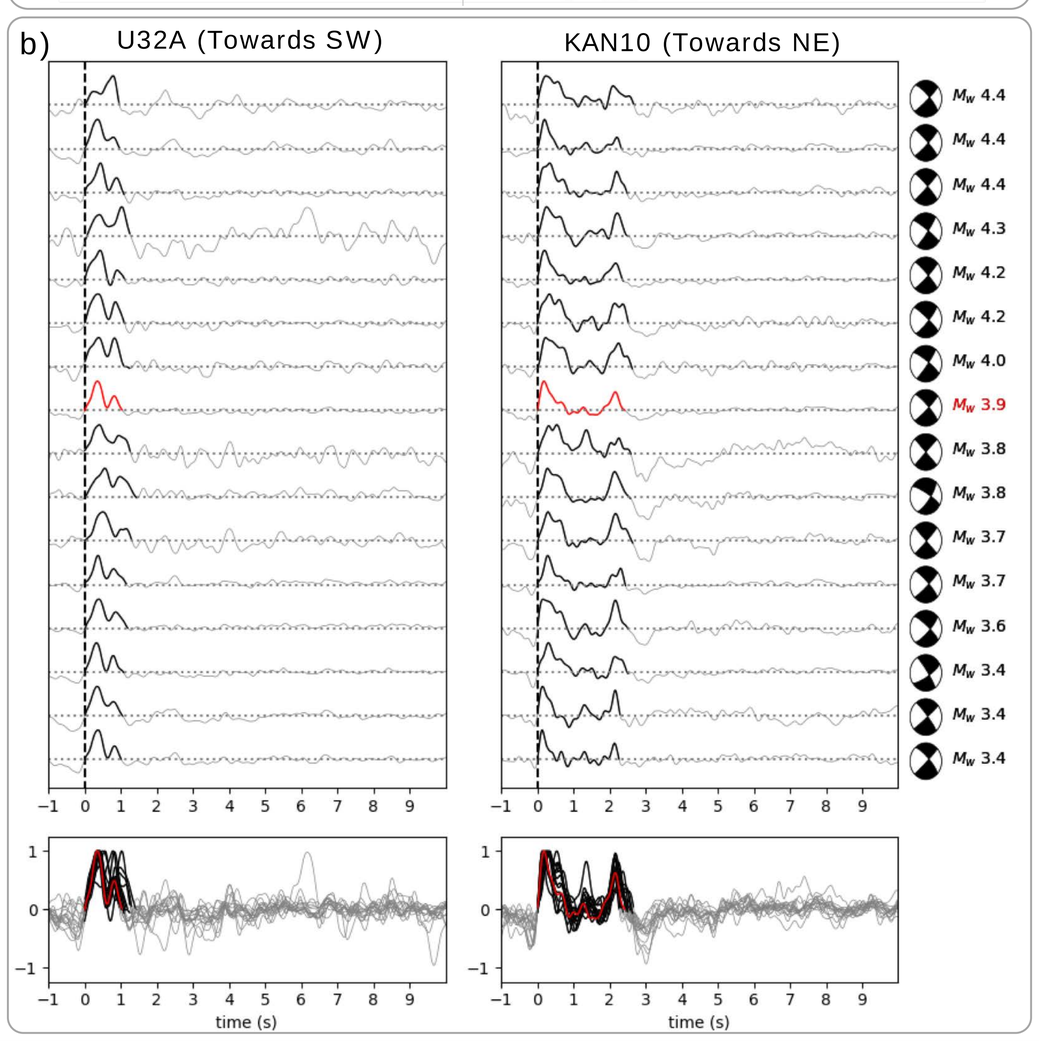

Figure 2. a) Empirical Green's Function (EGF) technique (figure from Lui and Huang, 2019). b) ASTFs for the 2016 M_w 5.1 Fairview, Oklahoma earthquake for two seismic stations at SW direction, U32A (left) and NE direction, KAN10 (right), using 16 different foreshocks and aftershocks as EGFs having depths (±3 km) and faulting geometries (±13° for the strike of the preferred plane) similar to the ones found for the main event.

3. RUPTURE COMPLEXITY

- Two source pulses slightly separated are easily identified at NE azimuths, while stations located toward SW record single pulses of overall shorter durations (Figure 3). Resulting apparent durations exceed empirical values resolved for M_w 5.1 earthquakes, which are typically about 1 s, suggesting two subevents separated in space and time.
- A new approach based on relative hypocenter-centroid location is developed in order to infer the relative location for the two subevents identified from the ASTF analysis (Figure 4).

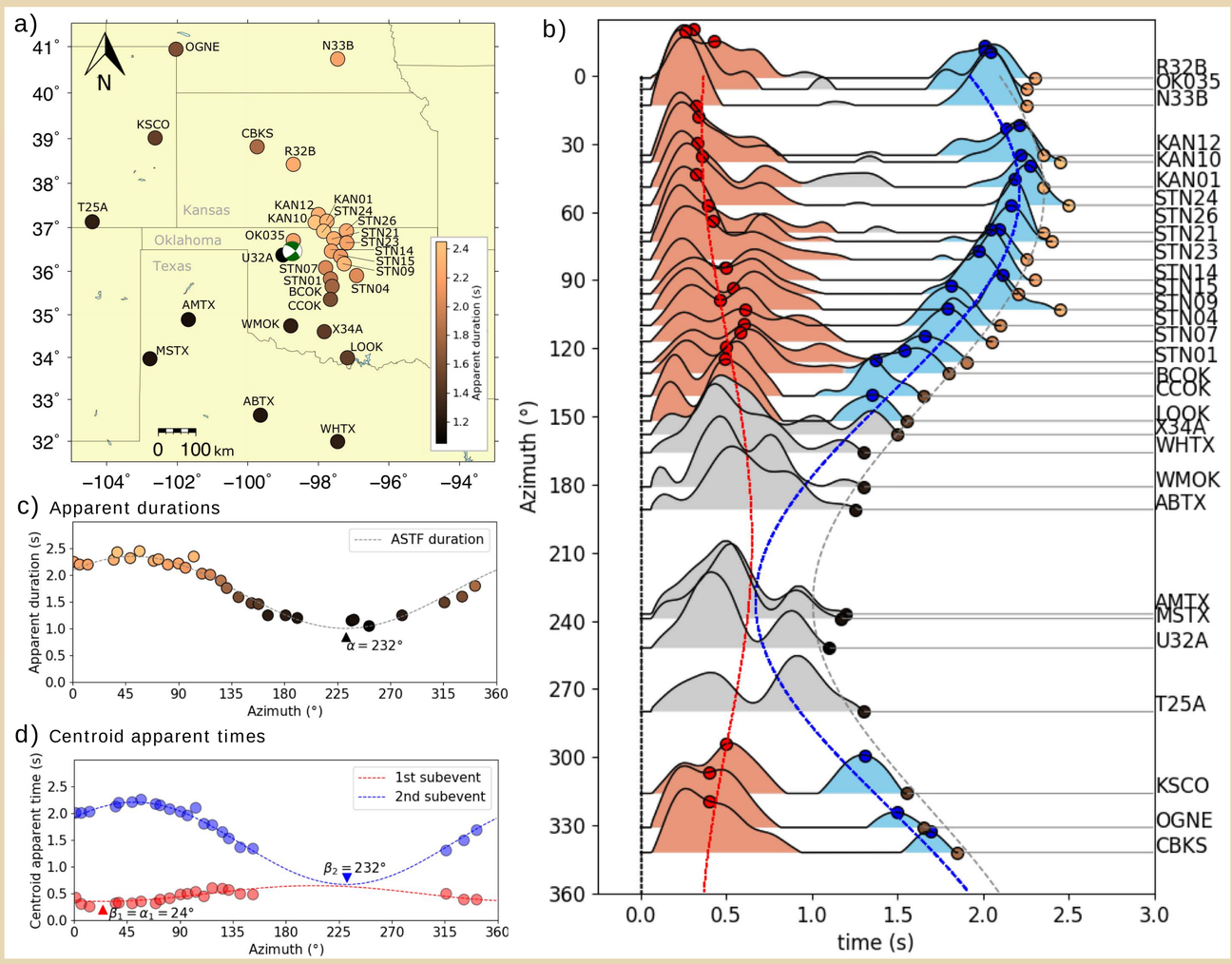

Figure 3. a) Map of near-regional seismic stations showing the apparent durations. b) ASTFs for each seismic station identifying each pulse associated with the first subevent (red area) and second subevent (blue area), excluding the traces where these pulses are overlapped and the contribution for each subevent is not evident (gray area). c) Inversion of apparent durations using Eq. 1. d) Inversion of centroid apparent times for each subevent using a full-grid search (Eq. 2).

➢ Apparent durations: $\tau(\phi) = t_R - \frac{L_R}{v_{P,S}}\cos(\phi - \alpha)$ (Eq. 1)

$\tau(\Phi)$ = Apparent duration as a function of the azimuth (Φ)
t_R = Rupture time
L_R = Rupture length
α = Azimuth of rupture directivity

➢ Centroid apparent times: $\tau_{Ci}(\phi) = \Delta t_i - \frac{d_j \cos\delta}{v_{P,S}}\cos(\phi - \beta_i)$ (Eq. 2)

$\tau_{Ci}(\Phi)$ = Centroid apparent times as a function of azimuth (Φ)
Δt_i = Delay time between the centroid location of each subevent and the origin time
d_j = Distance from the centroid and the hypocenter location (index j indicates each grid point defined on the fault plane)
β_i = Azimuth of each subevent centroid with respect to hypocentre ($\beta_1 = \alpha_1$)

- Fixed parameters: V_S = S-wave velocity (3.5 Km/s)
  δ = dip (70°)

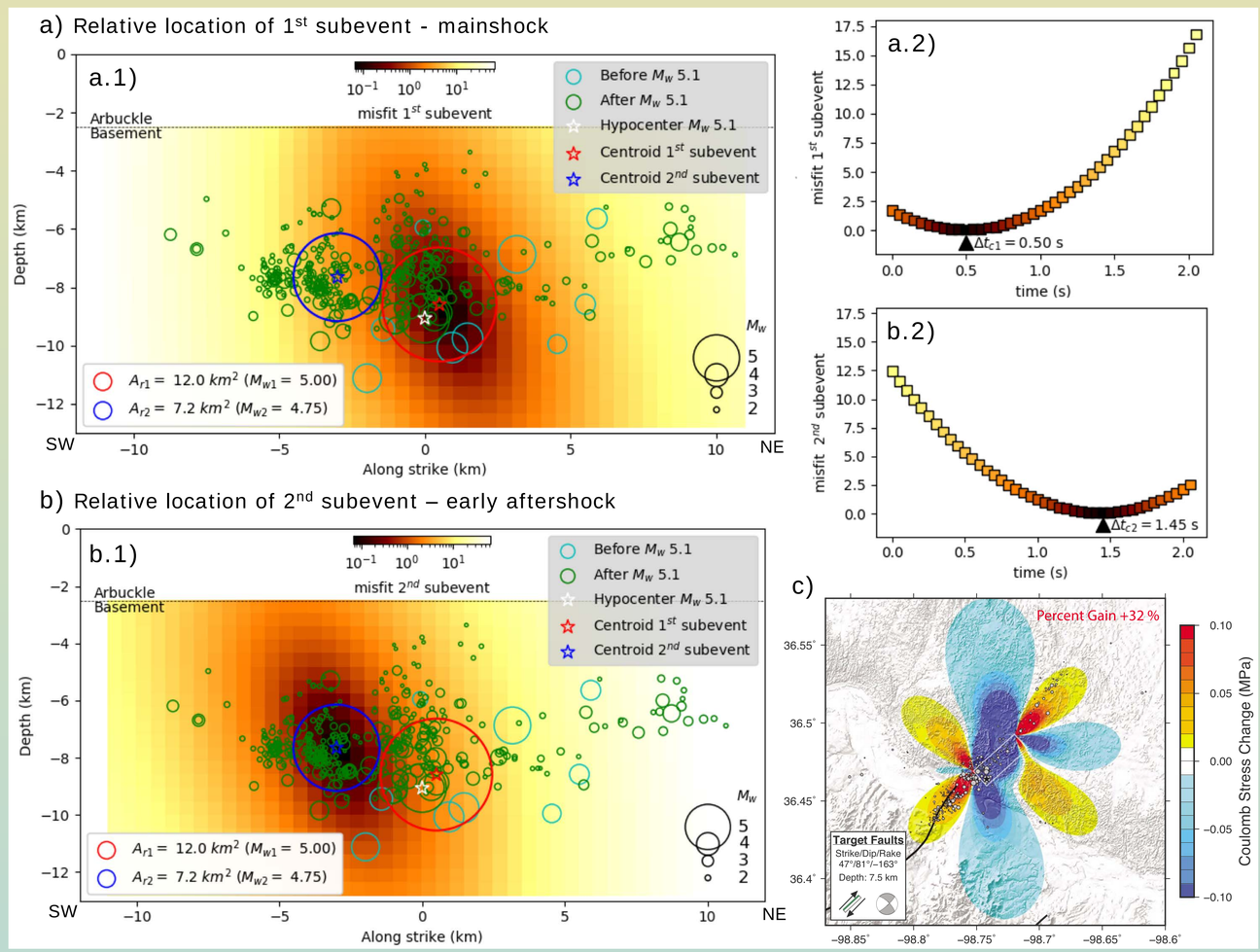

Figure 4. Relative hypocenter-centroid location for the first (a) and second (b) subevent. (a.1, b.1) A cross-sectional profile along the strike (B-B', figure 1b) showing the misfit as a function of the centroid location for each subevent. (a.2, b.2) Misfit for the delay time between the centroid location of each subevent and the origin time, Δt_i. (c) Coulomb failure stress change (ΔCFS) model estimated by Yeck et al., 2016.

4. CONCLUSIONS

➢ Rupture complexity of the Fairview earthquake involved a double event and rupture directivity effects in opposite directions.

➢ The first subevent has a magnitude of M_w 5.0 showing the main rupture propagation toward NE, in direction of the higher pore pressure perturbation due to wastewater injection.

➢ The second subevent appears as an early aftershock with lower magnitude M_w 4.7. It is located SW of the mainshock in a region of increased Coulomb stress, where most aftershocks were relocated.

REFERENCES

- López-Comino, J. A., & Cesca, S. (2018). Source complexity of an injection induced event: The 2016 Mw 5.1 Fairview, Oklahoma earthquake. *Geophys. Res. Lett.*, 45, 4025–4032.

- Goebel, T. H. W., Weingarten, M., Chen, X., Haffener, J., & Brodsky, E. E. (2017). The 2016 Mw 5.1 Fairview, Oklahoma earthquakes: Evidence for long-range poroelastic triggering at >40 km from fluid disposal wells. *Earth and Planetary Science Letters*, 472, 50–61.

- Yeck, W. L., Weingarten, M., Benz, H. M., Mcnamara, D. E., Bergman, E., Herrmann, R. B., Rubinstein, J. L., & Earle, P. S. (2016). Far-field pressurization likely caused one of the largest injection induced earthquakes by reactivating a large preexisting basement fault structure, *Geophys. Res. Lett.*, 43, 10,198–10,207.